Monatshefte für Chemie - Chemical Monthly (2022) 153:237–243
https://doi.org/10.1007/s00706-022-02897-w

ORIGINAL PAPER

The role of dye's structure on the degradation rate during indirect anodic oxidation

Gabriela Kuchtová[1] · Petr Mikulášek[1] · Libor Dušek[1]

Received: 16 December 2021 / Accepted: 31 January 2022 / Published online: 18 February 2022
© Springer-Verlag GmbH Austria, part of Springer Nature 2022

Abstract

The aim of this work was to evaluate the possibility of decolorization of effluents that contain structurally different azo and aminoantrachinone dyes. The decolorization was performed by an indirect electrochemical oxidation in a single-chamber laboratory electrolyzer under galvanostatic mode. Anodes used for the treatment were a planar boron-doped diamond and a platinum electrode. The changes in decolorization rate of model solutions were measured during indirect electrochemical oxidation in dependence on different initial pH in the presence of sodium sulfate, which is frequently used during the dyeing process. The decolorization process was compared with another abundant salt, specifically sodium chloride. The time intervals corresponding to chromaticity change of electrolyzed solution were measured and kinetic constants were assessed. Results showed that the decolorization rate is higher in the presence of NaCl than Na_2SO_4 and the structure of the dye has a direct impact on the velocity of the decolorization process. However, the degradation evaluated by the determination of total organic carbon parameter showed promising results also in the presence of sulfates on the boron-doped diamond anode dropping from 104 to 21 mg dm^{-3}. Since this parameter decreased on Pt anode only to 98 mg dm^{-3}, boron-doped diamond anode showed better performance in the presence of sulfates.

Graphical abstract

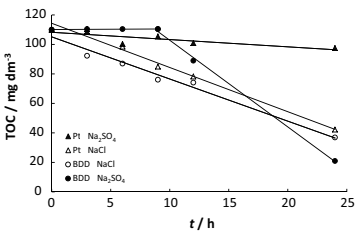

Keywords Boron-doped diamond · Electrochemistry · Decolorization · Degradation · Textile dyes

Introduction

Anodic oxidation attracts attention because of its potential to turn harmful substances into non-hazardous or low-toxicity chemicals. Unlike Fenton, photo-Fenton, ozone treatment, and other advanced oxidation processes it can operate under mild conditions, without chemical additives, formation of sludge and with an easiness of automatization [1, 2]. A connection with sources of renewable energy poses significant advantage, too [3, 4].

Due to outstanding properties like a wide potential window for water electrolysis, high mechanical and chemical stability, non-selective oxidation of organics, the boron-doped diamond (BDD) electrodes seem suitable for the treatment of different wastewaters [5, 6]. It has been proven that on the surface of boron-doped diamond electrodes not only a direct electron transfer and hydroxyl radical formation occur, but also the formation of sulfate oxidants [7, 8].

✉ Libor Dušek
libor.dusek@upce.cz

[1] Institute of Environmental and Chemical Engineering, University of Pardubice, Pardubice, Czech Republic

In the presence of sulfates in acidic pH, the reactions of sulfuric acid and its hydrogen ion with hydroxyl radicals take place to form sulfate radicals as shown in reactions (1) and (2), respectively [8, 9]. Sulfate radicals have a comparable oxidation potential ($E^\circ = 2.5–3.1$ V vs. NHE) to hydroxyl radicals ($E^\circ = 1.89–2.72$ V vs. NHE) but their half-life is by magnitudes higher. Specifically, 30–40 µs for sulfate radicals and 10^{-3} µs for hydroxyl radicals [10]. On the other hand, the mechanism of bond disruption is more selective for sulfate radicals [11], but they are efficient in a wider pH range (2–9) compared to hydroxyl radicals.

$$HSO_4^- + \bullet OH \rightarrow SO_4^{\bullet -} + H_2O \quad (1)$$

$$H_2SO_4 + \bullet OH \rightarrow SO_4^{\bullet -} + H_3O^+ \quad (2)$$

On the opposite side of the pH scale, direct oxidation of sulfate ion is preferred (3) [9]. The emerging sulfate radicals can easily react with hydroxyl ions and give rise to hydroxyl radicals, while the sulfate ion is being restored (4) [7]. The reaction rate of hydroxyl ions with sulfate radicals $1.4–8.3 \times 10^7$ M^{-1} s^{-1} exceeds the reaction rate with hydroxyl radicals $1.2–1.3$ 10^7 M^{-1} s^{-1}, thus the degradation of organics in alkaline condition is executed mainly by the action of hydroxyl radicals.

$$SO_4^{(2-)} - e^- \rightarrow SO_4^{(\cdot -)} \quad (3)$$

$$SO_4^{\bullet -} + {}^-OH \rightarrow SO_4^{2-} + \bullet OH \quad (4)$$

In all cases, the sulfate radicals are prone to form less potent peroxodisulfate (5). Despite its lower oxidation potential, it may participate in oxidation of organics after its activation [7, 12, 13]. The sulfate radicals can also promote the formation of hydroxyl radicals through reaction with water (6) or react with them to form less potent peroxymonosulfate (7) [14].

$$SO_4^{\bullet -} + SO_4^{\bullet -} \rightarrow S_2O_8^{2-} \quad (5)$$

$$SO_4^{\bullet -} + H_2O \rightarrow SO_4^{2-} + \bullet OH + H^+ \quad (6)$$

$$SO_4^{\bullet -} + \bullet OH \rightarrow HSO_5^- \quad (7)$$

There have already been published studies devoted to application of electrochemical processes to treat real wastewater [15–17]. The indirect oxidation has been used for the pesticides [18, 19], pharmaceuticals [20–22], even the dyes [23, 24]. The characteristics of effluent containing dyes may vary greatly not only across different industries (textile, paper, production of dyes, etc.) but also in the different stages or seasons within the same industry, therefore, the typical example of such water is difficult to define. An example of such water can be found in textile industry effluents, where pH usually ranges from 5.5 to 11.8 and the content of salt is mostly in the order of 0.1–10 g dm^{-3} [25].

With this work, we would like to assess the potential of the indirect anodic oxidation in the presence of sulfates for the decolorization of structurally different dyes and the influence of the dye's structure on the kinetics of the process in different conditions.

Results and discussion

Since many available technologies for water treatment are strongly dependent on initial pH, like Fenton or biological processes, the influence of initial pH on the decolorization process was evaluated. It was characterized by average kinetic constants of pseudo-first order calculated by Eq. (8).

$$kt = \ln\frac{[\text{dye}]_0}{[\text{dye}]_t} = 2.303\log\frac{[\text{dye}]_0}{[\text{dye}]_t}. \quad (8)$$

The calibration curve of absorbance at the maximum wavelength in dependence of known concentration for Direct Blue 71 (DB71), Direct Orange 102 (DO102), Direct Yellow 44 (DY44), Direct Red 80 (DR80), Acid Green 25 (AG25), Acid Red 118 (AR118), and Acid Blue 80 (AB80) was constructed according to Lambert–Beer's law at first. Then, the actual concentration of a dye was obtained from the absorbance recorded in time intervals lasting 2 or 5 min.

Even though the pH value can be controlled in laboratory conditions, the fluctuating character of real wastewater makes the control over pH difficult. From the technological point of view, the applicability of this approach is more appealing when the pH value is not corrected. As

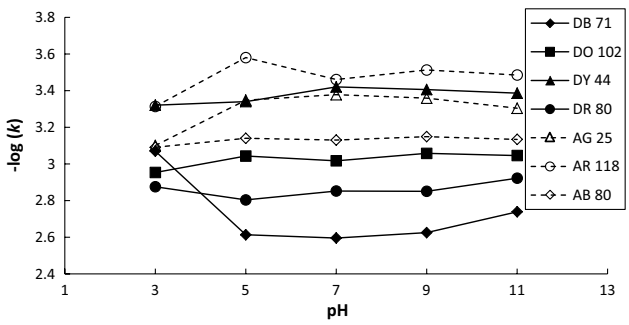

Fig. 1 Dependence of kinetic constant on initial pH of structurally diverse dyes measured during electrolysis of model solution on BDD anode with constant $I = 0.16$ A in the presence of sulfates with $c_0 = 7.28$ g dm^{-3}, $V = 0.25$ dm^3, $T = 25$ °C

can be seen on Fig. 1, the decolorization differs mostly in a strongly acidic area. Longer time is needed for the destruction of a chromophore and can be noticed mainly for Direct Blue 71. The experiment was carried out repeatedly to exclude accidental error. The average kinetic constant was 8.7178×10^{-4} s^{-1} with standard deviation 1.9623×10^{-5}. On the other hand, under these conditions acid dyes, which are exhausted from weak acid baths during the application on textile fibres, can be decolorized in shorter periods. In the acidic pH 3, the shift to the alkaline region is very subtle. The final pH in this area ranged between 3.04 and 3.55. Contrarily, the final pH of all other initial pH values after decolorization shifted to 10.47 ± 0.69. The pH shift to the alkaline region was achieved in the range of minutes and alkaline surroundings remained also during the ongoing degradation. The reason behind this is most likely the formation of carbonate–bicarbonate buffer, which can cover the pH range 8.9–10.8 [26, 27]. Therefore, the initial pH had relatively insignificant impact on the kinetic constants.

Nonetheless, noticeable differences in the decolorization time expressed by the kinetic constants can be observed amongst the structurally different dyes. Overview of the kinetic constants obtained at comparable conditions is depicted in Fig. 2.

It is obvious that the direct dyes, except Direct Yellow 44, are more susceptible to chromophore disintegration than the acid dyes. As can be seen from the structure of Direct Yellow 44 on Fig. 3D, by the break of carbamoylamino binding, products absorbing at the same region as a parent compound can be formed. The kinetic constant might include not only the chromophore disintegration but also the degradation of intermediates that could result in lowering the value of apparent kinetic constant. Interestingly, even the structurally similar dyes like Acid Blue 80 and Acid Green 25 (Fig. 3A, B, respectively) do not react with the generated oxidants at the same speed. Kinetic constant for Acid Green 25 being 3.9849×10^{-4} s^{-1} and Acid Blue 80 being 7.4097×10^{-4} s^{-1}, which is almost 2 times higher. Explanation can be found

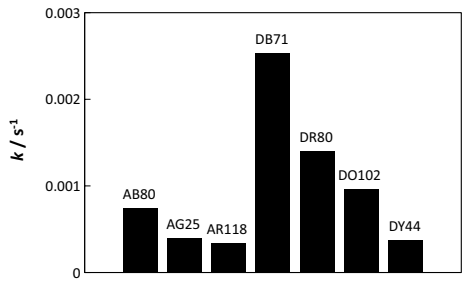

Fig. 2 Comparison of kinetic constants of structurally diverse dyes measured during electrolysis of model solution on BDD anode with constant $I = 0.16$ A in the presence of sulfates with $c_0 = 7.28$ g dm^{-3}, $V = 0.25$ dm^3, $T = 25$ °C and unadjusted $pH_0 = 6.93 \pm 0.12$

in the positive inductive effect of the methyl group. The electron density on the benzene ring of Acid Blue 80 is higher and the Hammett substituent constant σ of methyl group equals to − 0.069 for *meta* and − 0.170 for *para* position, therefore, the reactive radicals attack it more willingly [28]. Similarly, Direct Orange 102 and Direct Red 80 with kinetic constants 9.6168×10^{-4} and 1.4057×10^{-3} s^{-1} have the same core structure as can be seen on Fig. 3F, G, respectively. Therefore, the structure of organic pollutant plays an important role from the perspective of time and cost savings. However, the unselective character of anodic oxidation on BDD anode provides the disintegration even of structurally complex matrices due to the synergic effect of emerging hydroxyl and sulfate radicals (reactions 1–4 and 6).

The addition of salt leads to the increase of conductivity, which should be beneficial for the electrolytic process because of the decreased ohmic resistivity. Nonetheless, the increasing conductivity does not necessarily mean better performance of an electrolytic process as depicted in Fig. 4. The kinetic constant is rising until it reaches maximum speed at 7–9 g dm^{-3}, but it declines afterwards. This outcome implies that the concentration of salt above 7 g dm^{-3} seems superfluous. Higher concentration of sulfates presumably leads to prevailing parasitic reactions between radicals formed from salt ions which result in a decreased radical-pollutant reaction.

Not only the decolorization, but also the degradation was assessed through total organic carbon as it serves as a tool for estimation of organic load. The results clearly showed that this parameter declined slowly in the beginning, mainly on BDD anode in the presence of sulfate ions. However, after 24 h, it has reached even lower value 20.96 mg dm^{-3} than in the presence of chlorides 36.91 mg dm^{-3}. The invariable character in the first 10 h followed by a sharp decrease in the presence of sulfates indicates that the organic structure of a dye is only oxidized or degraded to smaller organic products without the release of CO_2. Therefore, the organic content in terms of organic carbon remains the same and the disintegration to inorganic carbon compounds can be observed at later stages of the electrolysis. In the case of chlorides, the oxidation is accompanied with the release of small inorganic compounds from the beginning, but with the ongoing chlorination, products that are more resistant to degradation may be formed which explain the lower decline of total organic carbon (TOC) parameter after 24 h in comparison to sulfates.

On the other hand, active Pt anode was insufficient in the degradation of organic matter in the presence of sulfates, as this parameter decreased only to 97.52 mg dm^{-3}. The initial value of total organic carbon was 110.4 mg dm^{-3}. It should be noted, that the active anodes in general do not lead to formation of sulfate-derived radicals unlike chloride derived radicals [29, 30]. Therefore, the slight decrease of

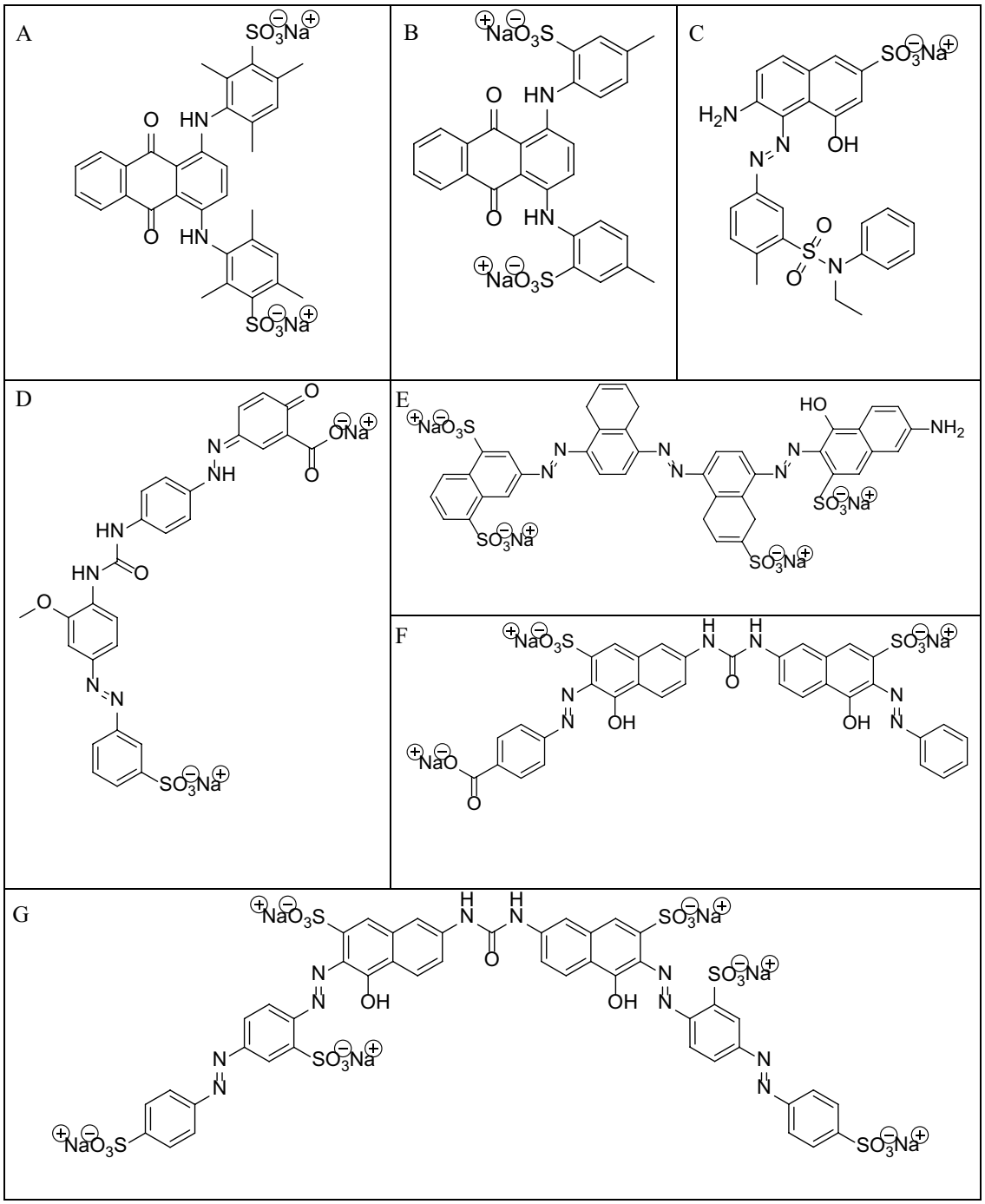

Fig. 3 Chemical structure of Acid Blue 80 (**A**), Acid Green 25 (**B**), Acid Red 118 (**C**), Direct Yellow 44 (**D**), Direct Blue 71 (**E**), Direct Orange 102 (**F**), and Direct Red 80 (**G**)

TOC corresponds to degradation caused by direct electron transfer and/or nonradical oxidation of a dye. Results are summarized in Fig. 5. Electric consumption reached 178 kWh m^{-3} for BDD in sulfates and 169 kWh m^{-3} in chlorides compared to 143 kWh m^{-3} and 137 kWh m^{-3} on platinum anode, respectively. However, in the presence of sulfates energy savings up to 35% can be achieved by the application of intermittent current supply [31].

The expenses can be also lowered by decreasing the interelectrode gap as can be seen in Fig. 6. In our laboratory, the construction of electrodes did not allow the distance from the center to center of the electrode to be lower than

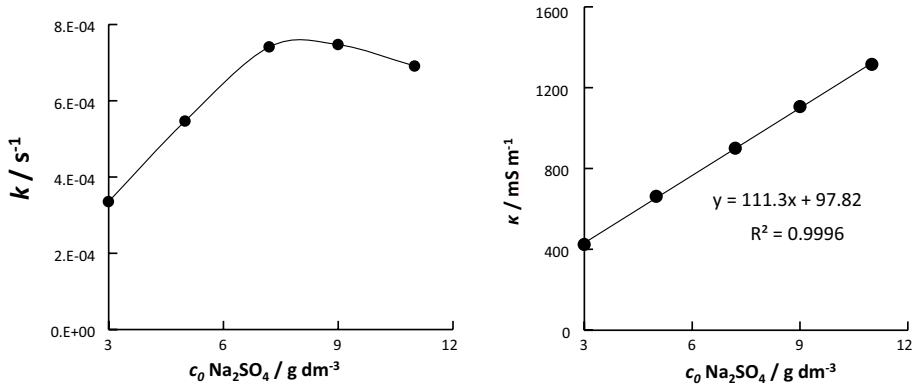

Fig. 4 Dependence of kinetic constant (left) and conductivity (right) on initial concentration of sodium sulfate measured during electrolysis of model solution with an initial concentration of AB80 = 1×10^{-4} mol dm^{-3}, $V = 0.25$ dm^3, $pH_0 = 6.35$, $T = 25$ °C on BDD anode with $I = 0.16$ A

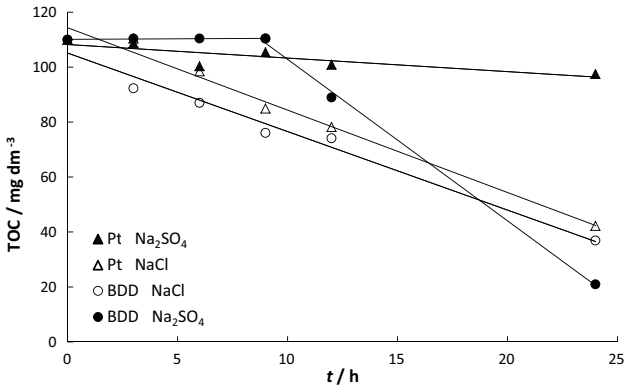

Fig. 5 Total organic carbon measured during electrolysis of model solution with initial concentration of Acid Blue 80 = 3×10^{-3} mol dm^{-3}, $V = 0.25$ dm^3, $pH_0 = 6.35$, $T = 25$ °C on platinum and BDD anode with $I = 0.16$ A in the presence of sulfates with $c_0 = 7.28$ g dm^{-3} and chlorides with $c_0 = 5$ g dm^{-3}

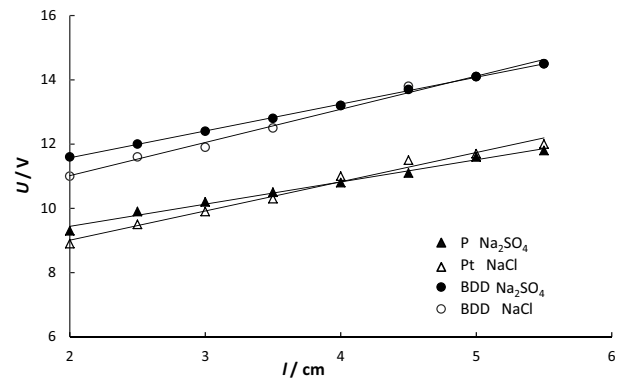

Fig. 6 Dependence of cell voltage on the electrode distance measured during electrolysis of model solution with initial concentration of sulfates $c_0 = 7.28$ g dm^{-3} and chlorides $c_0 = 5$ g dm^{-3}, $V = 0.25$ dm^3, $T = 25$ °C on platinum and BDD anode with constant $I = 0.16$ A

2 cm, but in the technological practice, smaller gap is achievable, which would cut the expenses even more.

Conclusion

This study demonstrates an amazing potential of electrochemical methods for the decrease of pollution in industrial wastewater containing resistant organic pollutants such as dyes. From the economical point of view, this process is suitable for wastewaters with organic load up to 5000 mg dm^{-3} of chemical oxygen demand (COD) [32, 33] as well as with enough salts to cause the drop in ohmic resistance. The application to wastewaters with high concentrations of chlorides should be minimised since the indirect anodic oxidation may contribute to the formation of toxic chlorinated by-products [29, 34, 35], therefore, wastewaters with naturally high content of sulfates are preferred. The conditions do have an impact on the process performance, however, all structurally complex compounds in this study were successfully disintegrated. The initial pH was adjusted quickly to the similar pH value, which is beneficial for industrial waters with fluctuating character, when the exact pH value may be hardly controllable. The structure of a compound plays a more important role. Even the small differences like a few methyl groups in a structure may hinder the degradation of a dye. Another crucial factor is the anode material and the presence of other compounds, mainly salts. Not only the nature of a salt, but also its concentration has an impact on the efficiency of the electrolysis. Herein, we showed that different organic compounds are susceptible to oxidation on BDD unlike Pt anode even during the mild conditions with the use of sulfates, that do not enhance the formation of halogenated organic compounds. The complementary action of emerging hydroxyl and sulfate radicals is beneficial for applicability of this technology across the whole pH range. Moreover, sulfate anions can be recycled on BDD anode during the electrolysis unlike chloride anions. With the prolonged electrolysis the TOC parameter decreased

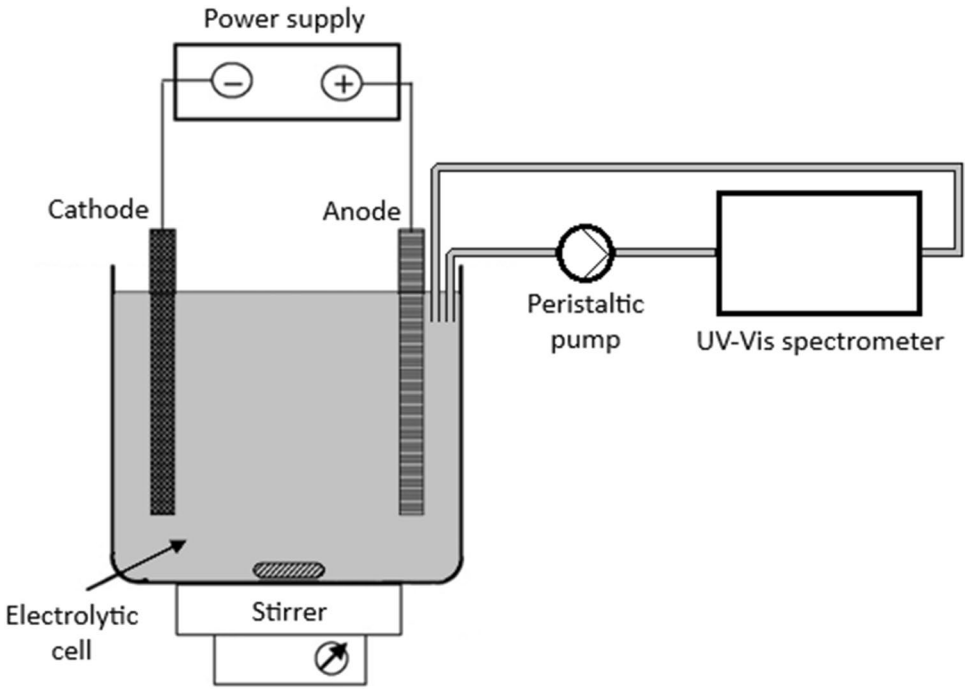

Fig. 7 Scheme of the experimental setup

significantly, but electric expenses were higher. However, intermittent current supply, narrow interelectrode gap or alternative sources of electrical energy may overcome this drawback in the future.

Experimental

The model wastewater was prepared by mixing distilled water, supporting electrolyte and a dye (Synthesis a.s., Czech Republic) with the initial concentration of textile dye Acid Blue 80, Acid Green 25, and Acid Red 118 equal to 1×10^{-4} mol dm^{-3} and paper dye Direct Blue 71, Direct Red 80, Direct Orange 102, Direct Yellow 44 with the initial concentration of 1.25×10^{-5} mol dm^{-3}. The initial concentration was chosen with regard to the opacity of the dye. The electrolyte, either sodium chloride ($c=5$ g dm^{-3}) or sodium sulfate ($c=7.3$ g dm^{-3}), was added to achieve a similar conductivity approximately 900 mS m^{-1}. The influence of pH was monitored in the presence of Na_2SO_4. The pH value was adjusted by addition of sodium hydroxide or sulfuric acid (Penta, s.r.o., Czech Republic), which were of analytical grade quality. All solutions were prepared in deionized water with the electrolytic conductivity about 1.0 µS cm^{-1} and correspond to resistivity ~ 1 MΩ cm (Milli-Q Plus system, Millipore, USA). Electrochemical oxidation was carried out in the single-chamber laboratory electrolytic cell with a volume of 0.25 dm^3 in the room temperature on a planar BDD anode (dimensions: 20×20 mm), described in detail in a previous monograph [29]. Figure 7 depicts the scheme of the experimental setup. Stabilized DC Power Supply Matrix MPS-3005 L-3 (Shenzen Matrix Technology Inc., China) was used for the electrolysis of the solution. The current was held constant at a value of 0.16 A. The electrolyzed solutions were stirred by magnetic stirrer Heidolph MR Hei-Tec (100 rpm). During electro-oxidation, the actual concentration of the dye was determined using UV–Vis spectrometer Libra S 22 (Biochrom Ltd., UK) according to Lambert–Beer law at the dye's maximum wavelength. The electrolytic cell was equipped with a closed circuit composed of peristaltic pump PP1B-05 (Zalimp, Poland), connecting tubes and 1 cm quartz flow cell located in the spectrophotometer. The degradation was monitored in the solution of Acid Blue 80 with the initial concentration 3×10^{-4} mol dm^{-3} on polished platinum sheet anode (dimensions: $10\times10\times0.4$ mm) or BDD anode. The cathode was made of austenitic stainless steel AISI 316 rod (dimensions: 30×3.5 mm) with a declared corrosion resistance in sea water. The total organic carbon was measured by a Formacs TOC/TN Analyzer (Skalar Analytical B.V., Nederland).

Acknowledgements We are grateful to prof. Ing. Ladislav Novotný, DrSc., Dr. for discussions and to the Student Grant Competition 2021 (SGS_2021_003) for financial support.

References

1. Nidheesh PV, Zhou M, Oturan MA (2018) Chemosphere 197:210
2. Comninellis CH, Kapalka A, Malato S, Parsons SA, Poulios I, Mantzavinos D (2008) J Chem Technol Biotechnol 83:769

3. Souza FL, Lanza MRV, Llanos J, Sáez C, Rodrigo MA, Cañizares P (2015) J Environ Manage 158:36
4. Chaplin BP (2014) Environ Sci Processes Impacts 16:1182
5. Hupert M, Muck A, Wang J, Stotter J, Cvackova Z, Haymond S, Show Y, Swain GM (2003) Diam Relat Mater 12:1940
6. Martínez-Huitle CA, Rodrigo MA, Sirés I, Scialdone O (2015) Chem Rev 115:13362
7. Farhat A, Keller J, Tait S, Radjenovic J (2015) Environ Sci Technol 49:14326
8. Divyapriya G, Nidheesh PV (2021) Curr Opin Solid State Mater Sci 25:100921
9. Chen L, Lei CH, Li Z, Yang B, Zhang X, Lei L (2018) Chemosphere 210:516
10. Olmez-Hanci T, Arslan-Alaton I (2013) Chem Eng J 224:10
11. Guerra-Rodríguez S, Rodríguez E, Singh DN, Rodríguez-Chueca J (2018) Water 10:1828
12. Song H, Yan L, Jiang J, Ma J, Zhang Z, Zhang J, Liu P, Yang T (2018) Water Res 128:393
13. Zhang T, Chen Y, Wang Y, Le Roux J, Yang Y, Croué JP (2014) Environ Sci Technol 48:5868
14. Giannakis S, Lin KYA, Ghanbari F (2021) Chem Eng J 406:127083
15. Mackuľak T, Vojs M, Grabic R, Golovko O, Vojs Staňová A, Birošová L, Medveďová A, Híveš J, Gál M, Kromka A, Hanusová A (2016) Monatsh Chem 147:97
16. Candia-Onfray CH, Espinoza N, Silva EBS, Toledo-Neira C, Espinoza LC, Santander R, García V, Salazar R (2018) Chemosphere 206:709
17. Bagastyo AY, Batstone DJ, Rabaey K, Radjenovic J (2013) Water Res 47:242
18. Domínguez JR, González T, Correia S (2021) J Environ Manage 298:113538
19. Ammar HB, Brahim MB, Abdelhédi R, Samet Y (2016) Sep Purif Technol 157:9
20. Murugananthan M, Latha SS, Raju GB, Yoshihara S (2011) Sep Purif Technol 79:56
21. Lan Y, Coetsier C, Causserand CH, Serrano KG (2017) Electrochim Acta 231:309
22. Radjenovic J, Petrovic M (2017) J Hazard Mater 333:242
23. Titchou FE, Zazou H, Afanga H, Gaayda JE, Akbour RA, Hamdani M, Oturan MA (2021) J Electroanal Chem 897:115560
24. Alcocer S, Picos A, Uribe AR, Pérez T, Peralta-Hernández JM (2018) Chemosphere 205:682
25. Yaseen D, Scholz M (2019) Int J Environ Sci Technol 16:1193
26. Delory GE, King EJ (1945) Biochem J 39:245
27. Boni JE, Brickl RS, Dressman J (2007) J Pharm Pharmacol 59:1375
28. Hammett LP (1937) J Am Chem Soc 59:96
29. Kuchtová G, Chýlková J, Váňa J, Vojs M, Dušek L (2020) J Electroanal Chem 863:114036
30. Song H, Yan L, Ma J, Jiang J, Cai G, Zhang W, Zhang Z, Zhang J, Yang T (2017) Water Res 116:182
31. Farhat A, Keller J, Tait S, Radjenovic J (2018) Electrochem Commun 89:14
32. Dušek L (2010) Chem Listy 104:846
33. Kapałka A, Fóti G, Comninellis CH (2008) J Appl Electrochem 38:7
34. Fabiańska A, Ofiarska A, Fiszka-Borzyszkowska A, Stepnowski P, Siedlecka EM (2015) Chem Eng J 276:274
35. Farhat A, Keller J, Tait S, Radjenovic J (2017) Chem Eng J 330:1265

Publisher's Note Springer Nature remains neutral with regard to jurisdictional claims in published maps and institutional affiliations.